energies

MDPI

Article

An Experimental and Kinetic Modeling Study of the Laminar Burning Velocities of Ammonia/*n*-Heptane Blends

Jinhu Liang [1,3], Anwen Wang [2], Yujia Feng [3], Xiaojie Li [2], Yi Hu [2], Shijun Dong [3,*], Yang Zhang [1,*] and Fengqi Zhao [1]

[1] National Key Laboratory of Energetic Materials, Xi'an Modern Chemistry Research Institute, Xi'an 710065, China; jhliang@nuc.edu.cn (J.L.); zhaofqi@163.com (F.Z.)
[2] State Key Laboratory of Coal Combustion, School of Energy and Power Engineering, Huazhong University of Science and Technology, Wuhan 430074, China; wangaw@hust.edu.cn (A.W.); d202180465@hust.edu.cn (X.L.); m202271100@hust.edu.cn (Y.H.)
[3] School of Environmental and Safety Engineering, North University of China, Taiyuan 030051, China; s202214042@st.nuc.edu.cn
* Correspondence: dongshijun@hust.edu.cn (S.D.); aerozy@163.com (Y.Z.)

Abstract: Ammonia is carbon-free and is a very promising renewable fuel. The ammonia/diesel dual-fuel combustion strategy is an important combustion strategy for ammonia internal combustion engines. To achieve clean and efficient combustion with a high ammonia blending ratio in ammonia engines, it is important to thoroughly investigate the combustion characteristics and chemical reaction mechanisms of ammonia/diesel fuel blends. Based on the constant volume combustion vessel experiments, the laminar burning velocities (LBVs) of ammonia/*n*-heptane blends were measured at the conditions of an ammonia–energy ratio of 60–100%, at initial pressures of 0.1–0.5 MPa and initial temperatures of 338–408 K, and under an equivalence ratio regime of 0.8–1.3. The experimental results indicate that the laminar burning velocities of ammonia/*n*-heptane fuel blends increase with a decreasing ammonia–energy ratio. Specifically, with an ammonia–energy ratio of 60%, an initial temperature of 373 K, an initial pressure of 0.1 MPa, and an equivalence ratio of 1.1, the measured LBV is approximately 20 cm/s, which is about 61% faster than that of pure ammonia flames under the same conditions. A previously developed chemical kinetic mechanism is employed to simulate the new experimental data, and the model exhibits overall good performance. The sensitivity analyses have been conducted to highlight the important reaction pathways. The elementary reaction $O_2 + \dot{H} <=> \ddot{O} + \dot{O}H$ demonstrates the most significant promotional effect on the laminar burning velocities, while the interaction reaction pathways of via H-abstraction from *n*-heptane by $\dot{N}H_2$ radicals are not showing obvious effects on the simulation results under the studied conditions.

Keywords: ammonia; laminar burning velocity; constant volume combustion vessel; kinetics modeling

Citation: Liang, J.; Wang, A.; Feng, Y.; Li, X.; Hu, Y.; Dong, S.; Zhang, Y.; Zhao, F. An Experimental and Kinetic Modeling Study of the Laminar Burning Velocities of Ammonia/*n*-Heptane Blends. *Energies* **2024**, *17*, 4874. https://doi.org/10.3390/en17194874

Academic Editor: Anastassios M. Stamatelos

Received: 5 September 2024
Revised: 19 September 2024
Accepted: 26 September 2024
Published: 28 September 2024

1. Introduction

Ammonia is carbon-free and does not generate CO_2 during combustion. It can be synthesized using renewable energy including solar and wind power. Additionally, ammonia facilitates storage and transportation at low cost [1]. Previous studies have shown that using ammonia in internal combustion engines can effectively reduce CO_2 emissions [2,3], making it an important technological approach for carbon reduction in the internal combustion engine industry.

Ammonia presents a higher octane number and a lower laminar burning velocity compared to traditional hydrocarbon fuels [1]. Thus, in the practical research of ammonia fuel engines, ammonia is often blended with more reactive fuels [1,4], including natural gas/methane [5], hydrogen [6], traditional diesel [7], and gasoline [8]. Previous studies have shown that the ammonia/diesel dual-fuel strategy is an important technical path for carbon emission reduction of marine engines. It is well known that *n*-heptane is usually

employed to represent diesel in engine combustion simulations, thus it is crucial to explore the fundamental combustion characteristics of ammonia/*n*-heptane blends in an engine under relevant conditions, including both the ignition delay times (IDTs) and laminar burning velocities (LBVs).

There are a number of experimental studies focusing on the LBV measurements of both ammonia and various ammonia fuel blends. Ronney et al. [9] measured the LBVs of ammonia using the spherical flame propagation method. Subsequently, Pfahl et al. [10], Jabbour et al. [11] used the spherical flame propagation method to measure the LBVs of both pure ammonia and different ammonia fuel blends at normal temperature and pressure conditions. However, the influence of the flame stretch rate was not considered in these experiments, which causes large uncertainties [12]. In recent years, new experiments at high initial temperatures and initial pressures have been conducted. Hayakawa et al. [13] performed an experimental study on the LBV and the Markstein length of ammonia/'air' mixtures at different pressures up to 0.5 MPa and equivalence ratios ranging from 0.7 to 1.3. Zhou et al. [14] performed an experimental and kinetic modeling study on laminar burning velocities of NH_3/'air', NH_3/H_2/'air', NH_3/CO/'air', and NH_3/CH_4/'air' mixtures in a constant volume combustion bomb, and a kinetic model was proposed to simulate these data. In addition, Han et al. [15,16] measured the LBVs of NH_3/'air' mixtures at initial temperatures ranging from 298–448 K using the heat flux method. Ichikawa et al. [17] performed an experimental and numerical simulation study on the LBVs of ammonia/hydrogen/'air' at pressures of 0.1–0.5 MPa. The experimental LBV results present a non-linear relationship with an increasing hydrogen ratio. Additionally, Zuo et al. [18] measured the combustion characteristics of NH_3/H_2/'air' flames with different N_2 dilution degrees and equivalence ratios using the spherical propagating flame method. The results indicated that the addition of nitrogen led to a decrease in the measured LBVs.

Lavadera et al. [19] performed experimental and numerical explorations using the heat flux method to investigate mixtures of ammonia with *n*-heptane, *iso*-octane, and methane. The ammonia fuel mole fraction changed from 0% to 90%, with initial temperatures of 298 K and 338 K and equivalence ratios from 0.7 to 1.4. The experimental results revealed that adding ammonia to *n*-heptane, *iso*-octane, and methane decreases LBVs. When the equivalence ratio was fixed, it was observed that the LBVs decreased non-linearly with an increase in the NH_3 ratio but exhibited an approximately linear relationship with the NH_3 mass fraction concentration. Furthermore, the effects of ammonia on the combustion speed of *n*-heptane and *iso*-octane were found to be essentially the same, but slightly higher for methane.

In particular, there is a lack of research on the LBVs of ammonia/*n*-heptane fuel blends at high ammonia–energy ratio, high-temperature, and high-pressure conditions. Therefore, this study experimentally investigated the laminar flame propagation speed of ammonia/*n*-heptane blended fuels at high ammonia blending ratios and different ambient temperature and pressure conditions. A previously proposed chemical mechanism was used to simulate these new data, and sensitivity analyses were performed to highlight the important reaction pathways.

2. Experimental Section

To explore the effects of different blending ratios, initial pressures and temperatures on the LBVs of ammonia/*n*-heptane blends, comprehensive experiments were conducted under different conditions, with ammonia–energy ratios of 60–100%, initial pressures of 0.1–0.5 MPa, initial temperatures of 338–408 K, and equivalence ratios of 0.8–1.3. The experimental conditions are given in Table 1. The operational steps during the experiment are as follows: to avoid experimental errors, each set of experimental conditions was tested at least three times to ensure reliability and accuracy of the results.

Table 1. Experimental conditions.

Test	Ammonia–Energy Ratio	Initial Pressure/ MPa	Initial Temperature/ K	Equivalence Ratio
1	100%	0.1	373	0.8–1.3
2	80%	0.1	373	0.8–1.3
3	60%	0.1	373	0.8–1.3
4	60%	0.1	338	0.8–1.3
5	60%	0.1	408	0.8–1.3
6	60%	0.2	373	0.8–1.3
7	60%	0.5	373	0.8–1.3

The experiments were performed in a visual constant-volume combustion vessel. The schematic diagram of the experimental setup is shown in Figure 1. A detailed description of the facility can be found in [20], thus a brief introduction is provided in this paper. This facility includes a constant-volume chamber, a gas supply and mixing tank system, an ignition system, and a data acquisition system. According to Dalton's law of partial pressures, the mixtures used in the experiments were prepared in the stainless-steel mixing tank and then maintained for more than 8 h. The flame images were captured using a MotionPro Y4-S1 high speed CCD camera, via the two quartz windows installed oppositely on the combustion vessel. The images were recorded at 20,000 fps with a resolution of 640 × 480 pixels. In the experiments, the camera was triggered before spark plug discharge.

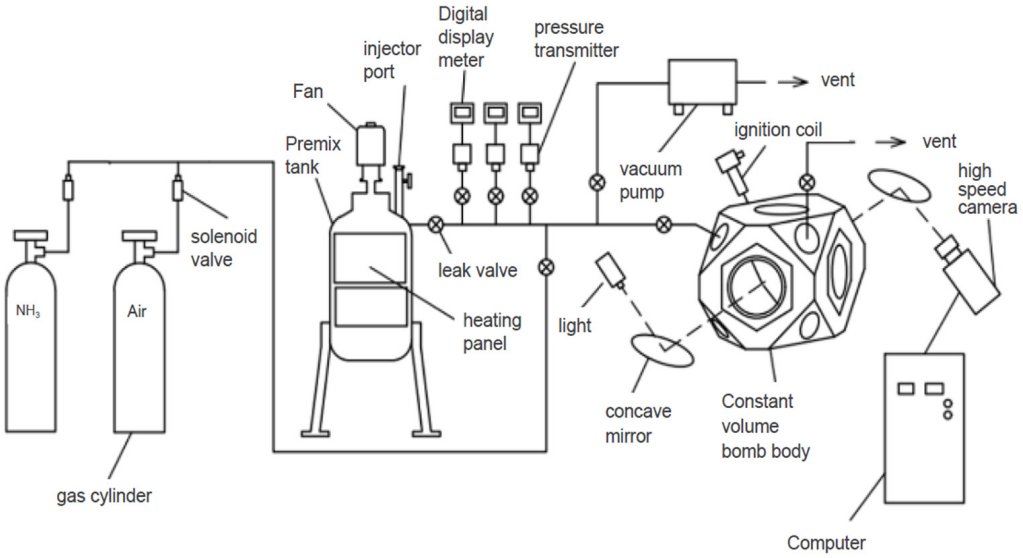

Figure 1. Experimental setup of the combustion vessel.

In this study, a MATALB code (R2024a) was used for image processing. The flame front was identified based on the significant variations in brightness between the flame front and its surroundings [21]. Each condition was repeated three times in the experiments. The methods of determining LBVs are the same as the previous study [22], and the relative error of the measured LBVs is 5%. Figure 2 shows the recorded images of flame propagating process of the ammonia/'air' mixture. For both 0.1 MPa and 0.2 MPa ambient pressures, it can be seen that the surfaces of the spherical flames are smooth during the flame propagation process. While for the 0.5 MPa ambient pressure, the flame propagation process presents cellular flame structures due to the increased pressure. The cellular flame structures can accelerate the flame propagation and hence results in faster measured flame speeds than actual values.

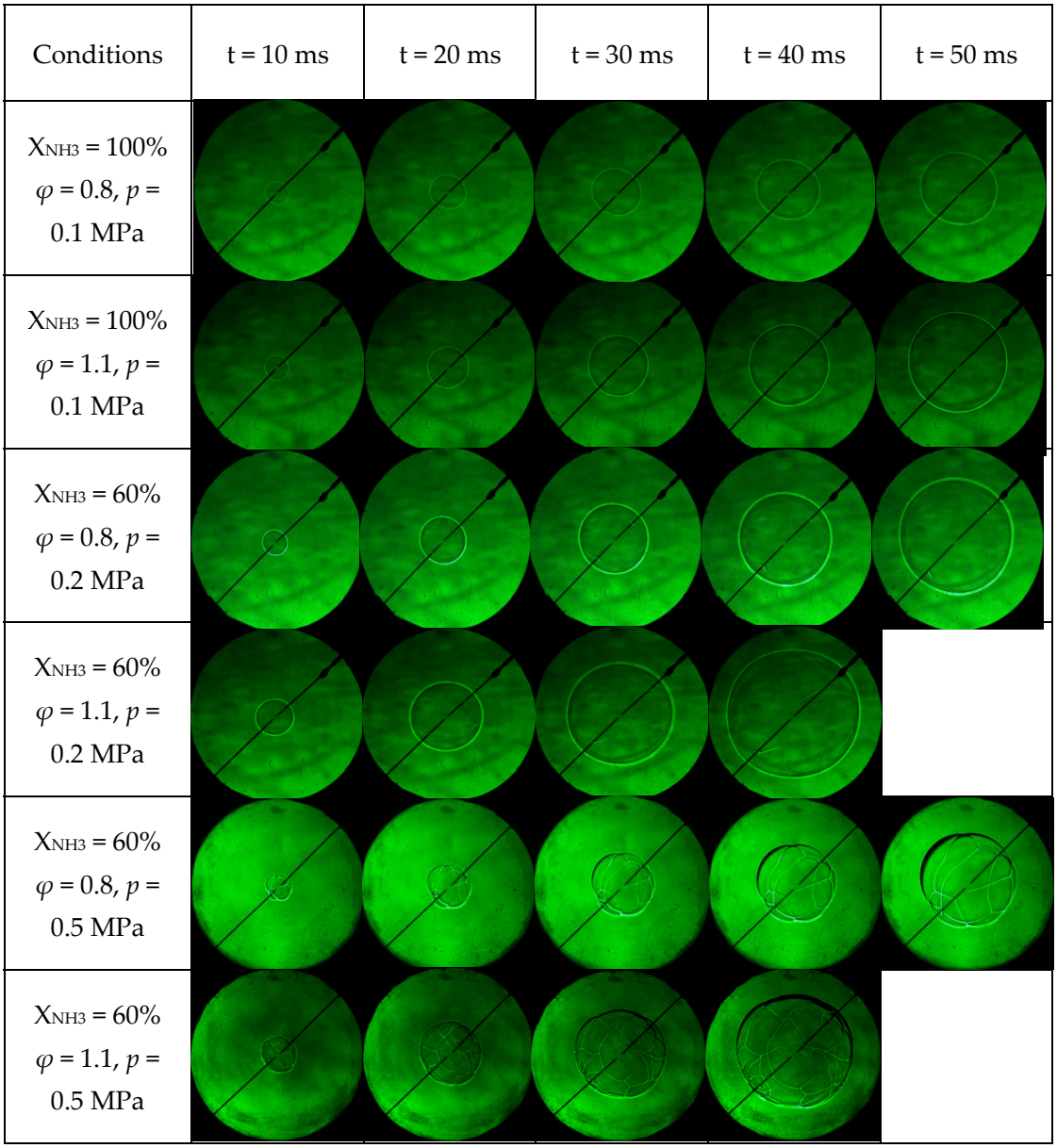

Figure 2. Spherical flame propagating process of ammonia and ammonia/*n*-heptane blends at an initial temperature of 373 K and different ambient pressures.

To validate the reliability of the experimental data based on the current facility, LBVs of the ammonia/'air' mixture were measured with the experimental conditions consistent with the study by Lhuillier et al. [23]. The LBV results measured using the current facility are compared with the experimental results of Lhuillier et al. [23] and the simulation results based on the mechanism of Dong et al. [24] are also plotted in Figure 3 for comparison. As can be seen, the current experimental results are about 5% larger than those measured by Lhuillier et al. [23], while the simulations match well with the measurements using the current facility. The mechanism has been well validated against measured LBVs of ammonia/*n*-heptane blends in previous studies [25]. Thus, it can be concluded that the experimental LBV results measured using the current facility are reliable.

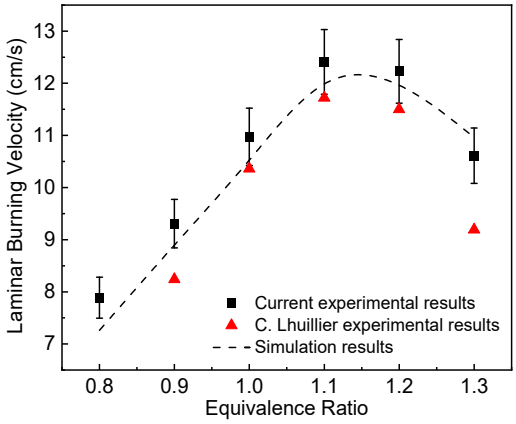

Figure 3. Comparisons of ammonia/'air' laminar burning velocities at different equivalence ratios with experimental results from Lhuillier et al. [23], at an initial pressure of 0.1 MPa and an initial temperature of 373 K. The simulation results are using the mechanism of Dong et al. [24].

3. Kinetic Modeling

The previously developed kinetic mechanism of ammonia/*n*-heptane blends was employed to simulate these new measured experimental data [24]. The NOx sub-chemistry in this reaction mechanism mainly comes from Glarborg et al. [25], and the interaction reaction pathway between NOx and C_1 to C_3 alkanes has been relatively well updated and validated [26,27]. During the model development, the key updated elementary reactions include high-temperature pyrolysis chemistry of ammonia taken from Alturaif et al. [28] and low-temperature oxidation chemistry of ammonia. These updates directly affect the simulations of laminar burning velocities of ammonia. Furthermore, the interaction reactions between ammonia and *n*-heptane have been included, i.e., H-atom abstraction from *n*-heptane via $\dot{N}H_2$ radicals. This mechanism has been well validated against comprehensive experimental data including IDTs and LBVs of ammonia/*n*-heptane blends under different conditions. All the simulations and the sensitivity analyses were conducted using CHEMKIN-PRO [29]. A closed homogeneous reactor model was used to simulate shock tube ignition delay experimental data.

4. Results and Discussions

4.1. Effects of Ammonia–Energy Ratios on the Laminar Burning Velocities of Ammonia/n-Heptane Blends

As discussed above, the LBVs of ammonia/*n*-heptane blends at different conditions were measured in this study, and the influences of the blending ratio, initial temperature, and initial pressure on the laminar burning velocities were investigated, respectively.

Figure 4 illustrates the effects of blending ratios on the LBVs of ammonia/*n*-heptane blends at equivalence ratios of 0.8–1.3, an initial pressure of 0.1 MPa, and an initial temperature of 373 K. The simulation results based on the previous mechanism [24] are also provided for comparison. It can be observed that with the same ammonia–energy ratio, the laminar burning velocities of ammonia/*n*-heptane blends initially increase and then decrease with an increasing equivalence ratio, and the laminar burning velocities reach maximum values at the equivalence ratio of 1.1 for all the fuel blends. As the ammonia–energy ratio decreases, the LBVs of ammonia/*n*-heptane blends gradually increase. When the ammonia–energy ratio decreases from 100% to 80%, the peak laminar burning velocity of ammonia/*n*-heptane blends increases by approximately 21%. When the ammonia–energy ratio decreases from 100% to 60%, the peak laminar combustion speed increases by approximately 61%. Comparatively, the blending ratio has larger effects on the LBVs in the fuel-lean regime than that in the fuel-rich regime.

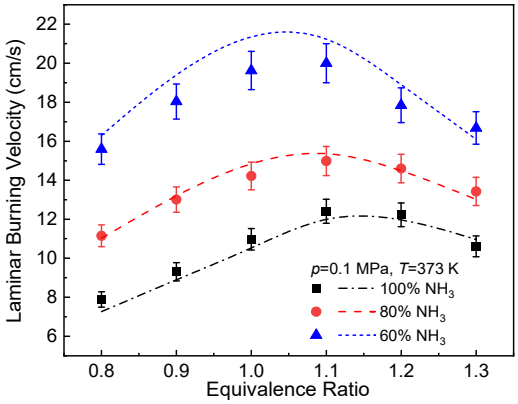

Figure 4. Effects of the blending ratio on the LBVs of ammonia/*n*-heptane blends, at an initial pressure of 0.1 MPa and an initial temperature of 373 K. The symbols represent the measured LBVs, and the solid lines represent the simulation results.

By comparing the experimental and simulated results, it can be seen that for different ammonia–energy ratios, the simulated results match reasonably well with the experimental results. Specifically, with ammonia–energy ratios of 100% and 80%, the simulated results match well with the experimental data under the equivalence ratio regime, and the deviations are within the error bar. With the ammonia–energy ratio of 60%, the experimental results are slightly overpredicted under the fuel-lean condition.

4.2. Effects of Ambient Temperatures on the Laminar Burning Velocities of Ammonia/n-Heptane Blends

Figure 5 illustrates the effects of ambient temperatures on the LBVs of ammonia/*n*-heptane blends (ammonia–energy ratio 60%) at equivalence ratios of 0.8–1.3 and at an initial pressure of 0.1 MPa. The simulation results are also plotted for comparison. Similarly, it can be observed that with different initial temperatures, the laminar burning velocities of ammonia/*n*-heptane blends initially increase and then decrease with an increasing equivalence ratio, and the laminar burning velocities reach maximum values at the equivalence ratio of 1.1 for all the temperature conditions. The experimental results show that the laminar burning velocities increase nonlinearly with the increasing initial temperature under the studied equivalence ratio regime. Specifically, with the initial temperature increasing from 338 K to 373 K, the laminar burning velocities only increase by approximately 4% in the studied equivalence ratio range. However, as the initial temperature increases from 373 K to 408 K, the laminar burning velocities increase by approximately 30% in the studied equivalence ratio range.

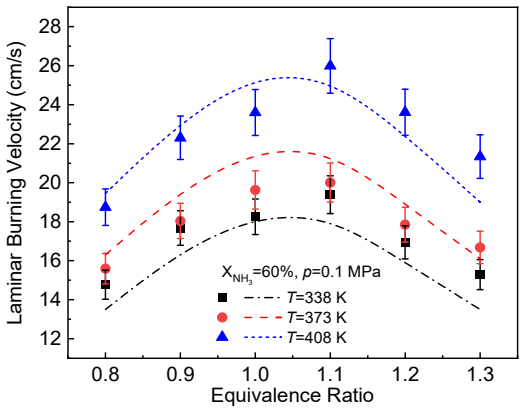

Figure 5. Effects of ambient temperatures on the LBVs of ammonia/*n*-heptane blends, with an ammonia–energy ratio of 60% and at an initial temperature of 373 K. The symbols represent the measured LBVs, and the solid lines represent the simulation results.

By comparing the experimental and simulated results, it is observed that the simulated results exhibit reasonably good consistency with the experimental trends at different initial temperatures. Specifically, the current model slightly underpredicts the LBVs at 338 K, while it overpredicts the LBVs at 338 K, with overall deviations of approximately 5–10% under the studied equivalence ratio regime. At 408 K, numerical simulation results match well with the experimental results under the studied equivalence ratio regime of 0.8 to 1.3.

4.3. Effects of Ambient Pressures on the Laminar Burning Velocities of Ammonia/n-Heptane Blends

Figure 6 shows the effects of ambient pressures on the LBVs of ammonia/*n*-heptane blends (ammonia–energy ratio 60%) at equivalence ratios of 0.8–1.3 and at an initial temperature of 373 K. By comparing the experimental and simulated results, it is observed that at initial pressures of 0.1 MPa and 0.2 MPa, the simulated results under the studied equivalence ratio regime match reasonably well with the experimental results. However, with the initial pressure of 0.5 MPa, the experimental results are significantly higher than the numerical simulation results, particularly for cases with equivalence ratios higher than 0.9. This discrepancy is primarily attributed to the appearance of cellular structures during the spherical flame propagation at 0.5 MPa. By examining the recorded images of the spherical flame propagation at different equivalence ratios, the results reveal more significant cellular structures at equivalence ratios of 1.0 and 1.1 than those at other equivalence ratios. As discussed in Section 2, the cellular flame structures of the spherical flames result in faster flame speeds. This indicates more pronounced acceleration effects on flame propagations at equivalence ratios of 1.0 and 1.1. This explains why the measured LBVs are higher than those of the simulation results.

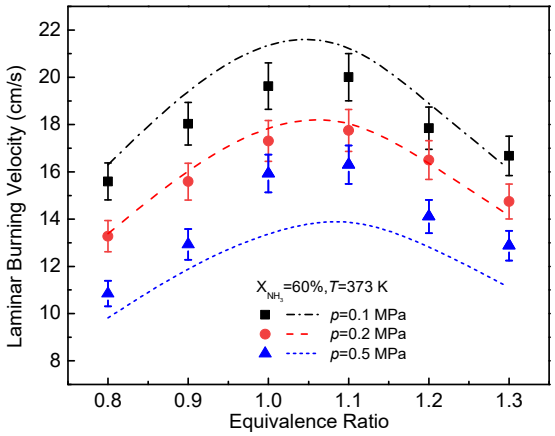

Figure 6. Effects of ambient pressures on the LBVs of ammonia/*n*-heptane blends, with an ammonia–energy ratio of 60% and at an initial temperature of 373 K. The symbols represent the measured LBVs, and the solid lines represent the simulation results.

Similarly, it can be observed that under different initial pressures, the laminar burning velocities of ammonia/*n*-heptane blends initially increase and then decrease with an increasing equivalence ratio, and the laminar burning velocities reach maximum values at the equivalence ratio of 1.1 for all the pressure conditions. The measured LBVs decrease with increasing initial pressures under the studied equivalence ratio regime. Specifically, when the initial ambient pressure increases from 0.1 MPa to 0.2 MPa, the peak laminar combustion speed decreases by approximately 11%.

4.4. Sensitivity Analyses

To further understand the chemistry that affects the flame propagation of ammonia/*n*-heptane blends under different conditions, sensitivity analyses have been performed using CHEMKIN-PRO [29] software. The sensitivity for the gas temperature with respect to A-factors has been calculated, and the results are given in Figure 7. The conditions

of the sensitivity analysis of ammonia/*n*-heptane laminar burning velocities were an ammonia–energy ratio of 60%, an initial pressure of 0.1 MPa, and an initial temperature of 373 K. The top ten elementary reactions with the greatest impacts of promoting and inhibiting flame propagating of ammonia/*n*-heptane blends are given for analyses. In Figure 7, positive and negative values indicate reactions promoting and inhibiting laminar burning velocities.

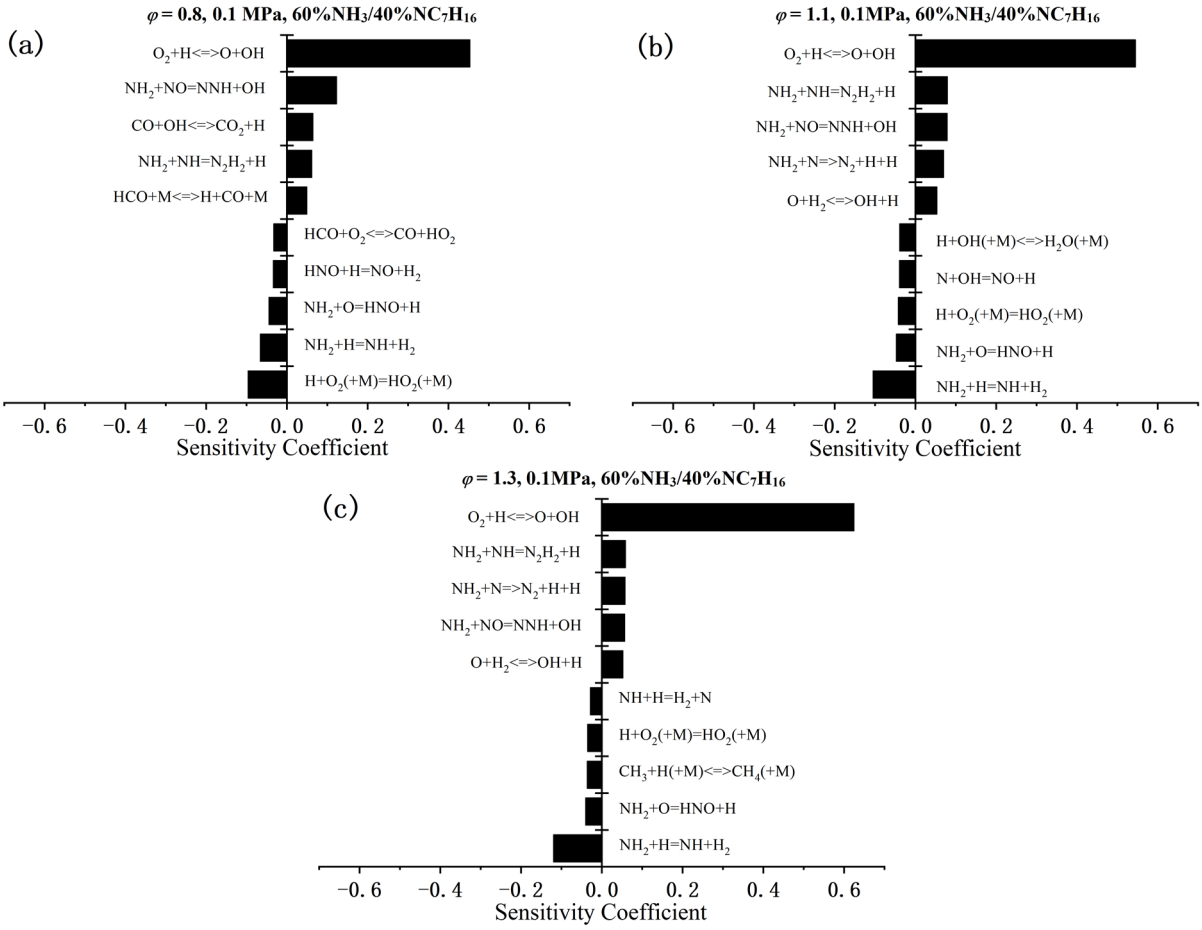

Figure 7. Sensitivity analysis results for LBVs of ammonia/*n*-heptane blends at different equivalence ratios, with an ammonia–energy ratio of 60% and at an initial temperature of 373 K.

The elementary reaction of O_2 + $\dot{H}$<=>$\ddot{O}$ + $\dot{O}H$ exhibits the greatest promoting impacts on laminar burning velocities of ammonia/*n*-heptane blends under all the studied conditions, and the sensitivity values are much larger than the other reactions. This reaction consumes one H atom and generates $\ddot{O}$ and $\dot{O}H$ radicals, and the $\ddot{O}$ radical can further react with H_2 to produce $\dot{O}H$ and $\dot{H}$ radicals. Therefore, this reaction significantly increases the concentration of reactive radicals. This is consistent with previous studies as this reaction is chain branching and produces H atoms, which is important for propagating flame. Moreover, the sensitivity values of this elementary reaction increase with increasing equivalence ratios; this is primarily due to the increased fuel concentration, which leads to an increased concentration of H atoms.

Also, it is evident that at different equivalence ratios, the elementary reactions that promote flame propagation form $\ddot{O}$, $\dot{H}$, and $\dot{O}H$ radicals, while the inhibiting reactions mainly consume these radicals and produce less reactive radicals. This indicates that these radicals can significantly accelerate the flame propagation of ammonia/*n*-heptane blends. Under the fuel-lean condition, the second most promoting reaction is $\dot{N}H_2$ + NO<=>NNH + $\dot{O}H$, while this reaction presents smaller promoting effects as the equivalence ratio increases.

This is because the increasing equivalence ratios lead to increased concentration of NH radicals, and this radical competes with NO via reacting with $\dot{N}H_2$ radicals. As can be seen, with increasing equivalence ratios, the reaction of $\dot{N}H_2$ + NH<=>N_2H_2 + $\dot{H}$ exhibits more significant promoting effects than that of $\dot{N}H_2$ + NO<=>NNH + $\dot{O}H$. Under fuel-rich conditions, the reaction of NH_2 + N=>N_2 + H + H also has a significant promoting effect; this is primarily due to the higher ammonia concentration under fuel-rich condition.

Among the elementary reactions that inhibit flame propagation, NH_2 + H<=>NH + H_2, H + O_2(+M)<=>HO_2(+M) and NH_2 + O<=>HNO + H consistently exhibit inhibiting effects under different equivalence ratios. Specifically, the sensitivity coefficient of NH_2 + H<=>NH + H_2 gradually increases with an increasing equivalence ratio, while the sensitivity coefficient of H + O_2(+M) <=>HO_2(+M) gradually decreases with an increasing equivalence ratio. The sensitivity coefficient of NH_2 + O<=>HNO + H initially increases and then decreases with an increasing equivalence ratio, indicating that the promoting effects of different elementary reactions on laminar combustion speeds vary with changes in the equivalence ratio. Under fuel-lean conditions, due to the lower fuel concentration, the primary inhibiting reactions involve the consumption of groups containing C and N fuel components, such as HCO and HNO. Therefore, under lean conditions, HNO + H<=>NO + H_2 and HCO + O_2<=>CO + HO_2 have a significant inhibiting effect on laminar combustion speeds. Under fuel-rich conditions, due to the higher fuel concentrations, the reaction of NH_2 + H<=>NH + H_2 has a greater inhibiting effect on flame propagation.

It is interesting to see that the reactions related to *n*-heptane decomposition and oxidation are not shown in Figure 7. This could be due to that the mole fraction of ammonia is about 95% in the fuel blends, which is much higher than that of *n*-heptane (~5%). Moreover, the important interaction reaction pathways of H-atom abstraction from *n*-heptane by $\dot{N}H_2$ radicals are not showing obvious sensitivities on the simulation results under the studied conditions. Under the fuel-lean condition, the most promoting reaction related to hydrocarbon chemistry is CO + $\dot{O}H$<=>CO_2 + $\dot{H}$, and this reaction consumes $\dot{O}H$ radicals while produces H atoms that can undergo chain branching by reacting with oxygen.

5. Conclusions

This paper experimentally measured the laminar burning velocities of ammonia/*n*-heptane blends using a constant volume combustion vessel, and the experimental conditions covered different blending ratios, ambient temperatures, and pressures at the equivalence ratios of 0.8–1.3. Numerical simulations and sensitivity analyses have also been conducted to understand the chemistry. The main conclusions are as follows.

The LBVs of ammonia/*n*-heptane/air increase with the decreasing ammonia–energy ratio, increasing initial ambient temperature, and decreasing initial ambient pressure. Specifically, with an ammonia–energy ratio of 60%, at an initial temperature of 373 K and an initial pressure of 0.1 MPa, the measured peak LBV is approximately 61% faster than that of pure ammonia flames under the same conditions. As the initial temperature increases from 373 K to 408 K, the LBVs increase by approximately 30% in the studied equivalence ratio range. As the initial ambient pressure increases from 0.1 MPa to 0.2 MPa, the peak LBV decreases by approximately 11%. The peak values of LBVs are observed at the equivalence ratio of 1.1 for all the studied conditions.

The comparisons of experimental and simulated results indicate reasonably good agreements at different ammonia–energy ratios, initial ambient temperatures, and pressures. Through sensitivity analyses, it is revealed that the reactions leading to the formations of $\dot{O}$ and $\dot{H}$ radicals have a strong promoting effect on laminar combustion speeds, with O_2 + $\dot{H}$<=>$\dot{O}$ + $\dot{O}H$ showing the greatest promoting effect on flame propagations of ammonia/*n*-heptane fuel blends.

This study explored the combustion characteristics of ammonia/*n*-heptane blends and the factors influencing flame propagations, contributing to a better understanding of the combustion of such fuel blends.

Author Contributions: Conceptualization, J.L. and S.D.; methodology, A.W.; validation, Y.F. and X.L.; investigation, J.L., A.W. and Y.H.; data curation, A.W. and Y.H.; writing—original draft preparation, J.L.; writing—review and editing, S.D. and Y.Z.; supervision, F.Z.; project administration, F.Z.; funding acquisition, J.L. All authors have read and agreed to the published version of the manuscript.

Funding: The authors would like to express their deepest appreciation for the support given by the Key Laboratory Fund of the Ministry of Public Security of the People's Republic of China (2023FMKFKT01), the National Natural Science Foundation of China (12172335), and the Scientific Activities of Selected Returned Overseas Professionals in Shanxi Province (20230014).

Data Availability Statement: Data are contained within the article.

Conflicts of Interest: The authors declare no conflict of interest.

References

1. Valera-Medina, A.; Xiao, H.; Owen-Jones, M.; David, W.I.F.; Bowen, P.J. Ammonia for power. *Prog. Energy Combust. Sci.* **2018**, *69*, 63–102. [CrossRef]
2. Reiter, A.J.; Kong, S.C. Combustion and emissions characteristics of compression-ignition engine using dual ammonia-diesel fuel. *Fuel* **2011**, *90*, 87–97. [CrossRef]
3. Dimitriou, P.; Javaid, R. A review of ammonia as a compression ignition engine fuel. *Int. J. Hydrogen Energy* **2020**, *45*, 7098–7118. [CrossRef]
4. Mounaïm-Rousselle, C.; Brequigny, P. Ammonia as Fuel for Low-Carbon Spark-Ignition Engines of Tomorrow's Passenger Cars. *Front. Mech. Eng.* **2020**, *6*, 1–5. [CrossRef]
5. Okafor, E.C.; Naito, Y.; Colson, S.; Ichikawa, A.; Kudo, T.; Hayakawa, A.; Kobayashi, H. Experimental and numerical study of the laminar burning velocity of CH_4–NH_3–air premixed flames. *Combust. Flame* **2018**, *187*, 185–198. [CrossRef]
6. Mørch, C.S.; Bjerre, A.; Gøttrup, M.P.; Sorenson, S.C.; Schramm, J. Ammonia/hydrogen mixtures in an SI-engine: Engine performance and analysis of a proposed fuel system. *Fuel* **2011**, *90*, 854–864. [CrossRef]
7. Reiter, A.J.; Kong, S.C. Demonstration of compression-ignition engine combustion using ammonia in reducing greenhouse gas emissions. *Energy Fuels* **2008**, *22*, 2963–2971. [CrossRef]
8. Grannell, S.M.; Assanis, D.N.; Gillespie, D.E.; Bohac, S.V. Exhaust emissions from a stoichiometric, ammonia and gasoline dual fueled spark ignition engine. In Proceedings of the ASME 2009 Internal Combustion Engine Division Spring Technical Conference, Milwaukee, WI, USA, 3–6 May 2009; pp. 135–141.
9. Ronney, P.D. Effect of Chemistry and Transport Properties on Near-Limit Flames at Microgravity. *Combust. Sci. Technol.* **1988**, *59*, 123–141. [CrossRef]
10. Pfahl, U.J.; Ross, M.C.; Shepherd, J.E.; Pasamehmetoglu, K.O.; Unal, C. Flammability limits, ignition energy, and flame speeds in H_2-CH_4-NH_3-N_2O-O_2-N_2 mixtures. *Combust. Flame* **2000**, *123*, 140–158. [CrossRef]
11. Jabbour, T.; Clodic, D.F. Burning velocity and refrigerant flammability classification. *ASHRAE Trans.* **2004**, *110*, 522–533.
12. Law, C.K.; Sung, C.J. Structure, aerodynamics, and geometry of premixed flamelets. *Prog. Energy Combust. Sci.* **2000**, *26*, 459–505. [CrossRef]
13. Hayakawa, A.; Goto, T.; Mimoto, R.; Arakawa, Y.; Kudo, T.; Kobayashi, H. Laminar burning velocity and Markstein length of ammonia/air premixed flames at various pressures. *Fuel* **2015**, *159*, 98–106. [CrossRef]
14. Zhou, S.; Cui, B.; Yang, W.; Tan, H.; Wang, J.; Dai, H.; Li, L.; ur Rahman, Z.; Wang, X.; Deng, S.; et al. An experimental and kinetic modeling study on NH_3/air, NH_3/H_2/air, NH_3/CO/air, and NH_3/CH_4/air premixed laminar flames at elevated temperature. *Combust. Flame* **2023**, *248*, 112536. [CrossRef]
15. Han, X.; Wang, Z.; Costa, M.; Sun, Z.; He, Y.; Cen, K. Experimental and kinetic modeling study of laminar burning velocities of NH_3/air, NH_3/H_2/air, NH_3/CO/air and NH_3/CH_4/air premixed flames. *Combust. Flame* **2019**, *206*, 214–226. [CrossRef]
16. Han, X.; Wang, Z.; He, Y.; Liu, Y.; Zhu, Y.; Konnov, A.A. The temperature dependence of the laminar burning velocity and superadiabatic flame temperature phenomenon for NH_3/air flames. *Combust Flame* **2020**, *217*, 314–320. [CrossRef]
17. Ichikawa, A.; Hayakawa, A.; Kitagawa, Y.; Kunkuma Amila Somarathne, K.D.; Kudo, T.; Kobayashi, H. Laminar burning velocity and Markstein length of ammonia/hydrogen/air premixed flames at elevated pressures. *Int. J. Hydrogen Energy* **2015**, *40*, 9570–9578. [CrossRef]
18. Zuo, S.; Chen, G.; Zhang, A.; Deng, H.; Wen, X.; Wang, F. Effect of diluent N_2 addition on NH_3/H_2/air combustion characteristics. *Fuel* **2023**, *352*, 129106. [CrossRef]
19. Lavadera, M.L.; Han, X.; Konnov, A.A. Comparative effect of ammonia addition on the laminar burning velocities of methane, n-heptane, and iso-octane. *Energy Fuels* **2021**, *35*, 7156–7168. [CrossRef]

20. Li, X.; Wang, Z.; Hu, Y.; Huang, Y.; Xiang, L.; Cheng, X. Experimental and numerical studies of the evaporation and combustion characteristics of large-angle impinging sprays. *Appl. Therm. Eng.* **2024**, *246*, 122918. [CrossRef]
21. Parsinejad, F.; Matio, M.; Metghalchi, M. A mathematical model for schlieren and shadowgraph images of transient expanding spherical thin flames. *J. Eng. Gas Turbines Power* **2004**, *126*, 241–247. [CrossRef]
22. Wu, Y.; Panigrahy, S.; Sahu, A.B.; Bariki, C.; Beeckmann, J.; Liang, J.; Mohamed, A.A.; Dong, S.; Tang, C.; Pitsch, H.; et al. Understanding the antagonistic effect of methanol as a component in surrogate fuel models: A case study of methanol/n-heptane mixtures. *Combust. Flame* **2021**, *226*, 229–242. [CrossRef]
23. Lhuillier, C.; Brequigny, P.; Contino, F.; Mounaïm-Rousselle, C. Experimental study on ammonia/hydrogen/air combustion in spark ignition engine conditions. *Fuel* **2020**, *269*, 117448. [CrossRef]
24. Dong, S.; Wang, B.; Jiang, Z.; Li, Y.; Gao, W.; Wang, Z.; Cheng, X.; Curran, H.J. An experimental and kinetic modeling study of ammonia/n-heptane blends. *Combust. Flame* **2022**, *246*, 112428. [CrossRef]
25. Glarborg, P.; Miller, J.A.; Ruscic, B.; Klippenstein, S.J. Modeling nitrogen chemistry in combustion. *Prog. Energy Combust. Sci.* **2018**, *67*, 31–68. [CrossRef]
26. Sahu, A.B.; Mohamed, A.A.E.-S.; Panigrahy, S.; Saggese, C.; Patel, V.; Bourque, G.; Pitz, W.J.; Curran, H.J. An experimental and kinetic modeling study of NOx sensitization on methane autoignition and oxidation. *Combust. Flame* **2022**, *238*, 111746. [CrossRef]
27. Mohamed, A.A.E.S.; Panigrahy, S.; Sahu, A.B.; Bourque, G.; Curran, H. The effect of the addition of nitrogen oxides on the oxidation of ethane: An experimental and modelling study. *Combust. Flame* **2022**, *241*, 112058. [CrossRef]
28. Alturaifi, S.A.; Mathieu, O.; Petersen, E.L. An experimental and modeling study of ammonia pyrolysis. *Combust. Flame* **2022**, *235*, 111694. [CrossRef]
29. CHEMKIN-PRO. *Reaction Design, version 15101*; Ansys: San Diego, CA, USA, 2010.